

Arrays of soliton waveguides in lithium niobate for parallel coupling

S. T. POPESCU*, A. PETRIS, V. I. VLAD, E. FAZIO^a

Natl. Institute for Laser, Plasma and Radiation Physics, Dept. of Lasers, Bucharest-Magurele, Romania

^aUniversity "La Sapienza" of Rome, Dept. of Energetics, Italy

Lithium niobate is a promising material for all-optical integrated photonics, particularly for soliton waveguides. An array of 13 x 10 soliton waveguides has been induced in a lithium niobate crystal using c.w. laser light at 532 nm wavelength. The spatial separation between waveguides (100 μm) ensures soliton writing without interactions, avoiding the possible deformation of soliton channels over a long distance (more than 15 diffraction lengths) and allowing the individual addressing of each soliton waveguide. The coupling and guiding properties of this parallel optical coupler at different wavelengths, with c.w. and pulsed laser signals, are investigated.

(Received December 15, 2009; accepted January 20, 2010)

Keywords: Soliton arrays, Parallel processing, Lithium niobate, Ultra-fast coupling

1. Introduction

Spatial bright solitons were previously demonstrated theoretically [1, 2] and experimentally [3] in photorefractive crystals. Nowadays, most experiments imply strontium barium niobate (SBN) [4, 5] and lithium niobate (LN) [6, 7], but other experimental demonstrations of solitons were made in barium titanate [8], bismuth silicon oxide [9, 10-13], nematic liquid crystals [14] or photonic crystals [15]. Screening photovoltaic soliton waveguides (SWG) were created by application of a strong external electrical field [6]. These SWGs created with visible light radiation were proved to support monomode propagation and good guiding of infrared wavelengths [16]. This fact makes them suitable for telecommunication applications. A big advantage of SWGs is their reconfigurability and the engineering process which is very simple and cheap.

SWG arrays were previously made in SBN [17, 18] showing the potential of ultra-fast and large bandwidth parallel processing. A 13x10 SWG array is demonstrated here in LN, material with low absorption, very low dispersion at telecommunication wavelengths and relatively cheap, since it is already widely used. In addition lithium niobate has already a niche in telecommunication market being used in modulators with frequencies of hundreds of GHz [19], due to its electro-optic properties. The guiding properties of this array are investigated at various c.w. wavelengths (532nm, 808nm, 1030nm, 1557nm) and ultra-short pulses (1030nm).

2. Experimental setup

For SWG writing, we have used an experimental setup similar to that shown in ref. [6], where the first

bright solitons were experimentally obtained in LN. Soliton writing and testing setup is shown in Fig. 1.

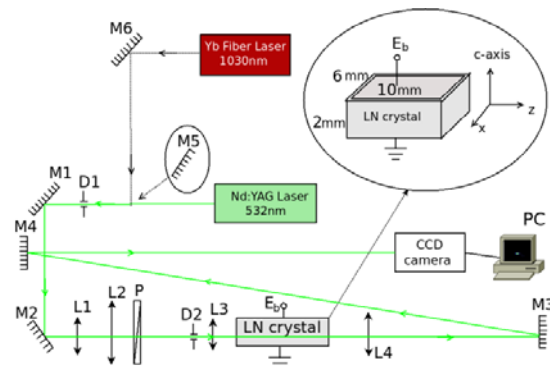


Fig. 1. Experimental setup for soliton waveguide writing and testing of the guiding properties.

A c.w. frequency doubled Nd:YAG laser ($\lambda=532$ nm) is used for the SWG writing. The beam is focused on the input face of the LN crystal with a FWHM spot diameter of 8 μm . A polarizer (P) was used to select the polarization of the input beam, parallel or orthogonal to the c-axis. The LN crystal is 2x6x10mm in size with the 10mm side (around 15 diffraction lengths) along the propagation direction, z. A high voltage is applied as in Fig. 1, in order to create a static electrical field along the c-axis of LN crystal. The time evolution of soliton formation and further propagation are visualized using a CCD camera connected to a computer. The camera and the image formation lens (L4) are positioned in such a way that images are magnified by a factor of 34. For the SWG guiding properties, the pump diode radiation (808 nm) and a weak intensity 532nm laser beam from the Nd:YAG laser are used. A Yb fibre laser is used to guide IR (1030

nm) c.w. and fs pulses (around 300fs) through the SWG. A c.w. telecom laser diode at $\lambda=1557\text{nm}$, was also used to test the guiding properties at this wavelength.

3. Soliton writing and erasing

Several tests were made to determine proper SWG writing conditions. The results presented here are for SWG written with extraordinary polarization of the incident beam. Background illumination was used in previous writing techniques [6]. The background illumination used in our case was the room light. We have measured the SWG writing time, t_w , for different bias electrical fields and for an input intensity $I=1500\text{W/cm}^2$ (an incident laser power of $750\mu\text{W}$). The experimental data are fitted with the exponential curve given by (Fig. 2):

$$t_w(E_b) = 1423 \cdot \exp(-0.087 \cdot E_b), \quad (1)$$

where E_b is the external bias field in kV/cm and t_w in minutes. This shows that increasing the external field from 40kV/cm to 50kV/cm , the SWG writing time is decreasing to half of its initial value (i.e. to 20 minutes).

The SWG writing time dependence of input beam intensity is shown in Fig. 3. The experimental dependence is fitted with the hyperbolic function:

$$t_w(I) = \frac{29.45}{I} + 4.67, \quad (2)$$

where the incident intensity, I is given in kW/cm^2 . From Fig. 3, one can observe that increasing the intensity above 1.5kW/cm^2 , the SWG writing time does not improve significantly.

The optimum conditions for SWG writing, considering the writing time and waveguide stability, were found for the input beam average power of $750\mu\text{W}$ ($I=1.5\text{kW/cm}^2$) and $E_b=47\text{kV/cm}$. The external bias field was limited to 50kV to avoid possible discharges near the crystal. A better insulation and better contacts could allow higher external voltages and speed up the writing process.

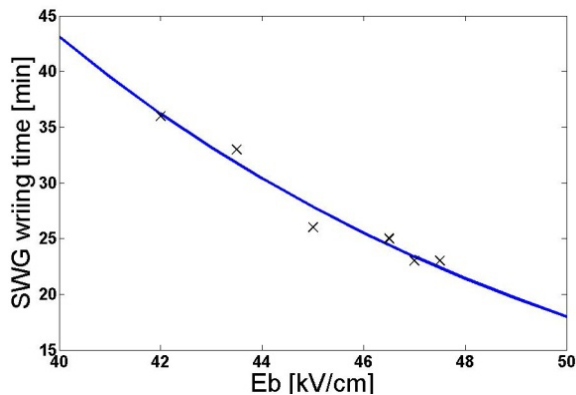


Fig. 2. SWG writing time function of the external bias field at input intensity of 1.5 kW/cm^2 .

For the mentioned conditions, the SWG writing time is around 24 minutes. The time evolution of beam profile during SWG writing is shown in Fig. 4.

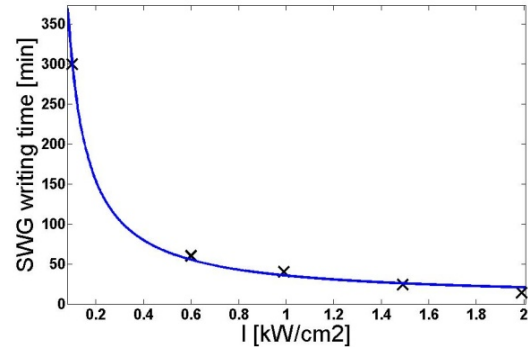


Fig. 3. SWG writing time function of the input beam intensity for a bias field of 47kV/cm .

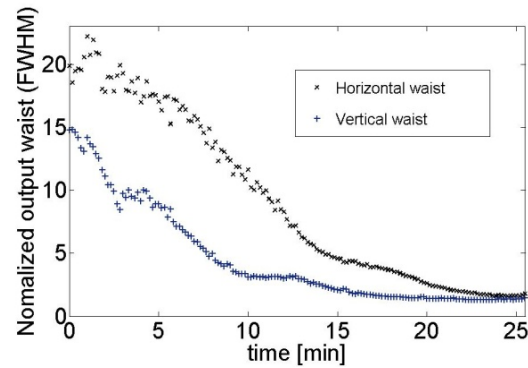


Fig. 4. Normalised output waist during SWG writing for both transversal directions.

As expected [6, 24], the beam is confining faster on the vertical direction (corresponding to the c-axis of the LN crystal). One can remark also that the writing time for a cylindrical (2D confined) soliton could be defined at the contact between the horizontal and vertical curves. The beam remains well confined on both transversal directions for a time interval of 1-3 minutes. Afterwards, a beam splitting process is starting on the horizontal direction (x-axis).

In Fig. 5, images of the beam self-confining process at different time steps are shown. The images are acquired on the output face of the LN crystal during the SWG writing.

The SWG obtained are slightly tapered (the average ratio between output and input waist at FWHM is around 1.5). This can be very useful for coupling applications. Beam bending [20] due to the charge diffusion was observed. It is around $30\mu\text{m}$ at the output crystal face, for our writing conditions. The erasing process of SWG was also investigated. This is accomplished by illuminating the crystal with a radiation wavelength in the photorefractive sensitivity range of LN crystals, which is from red to UV.

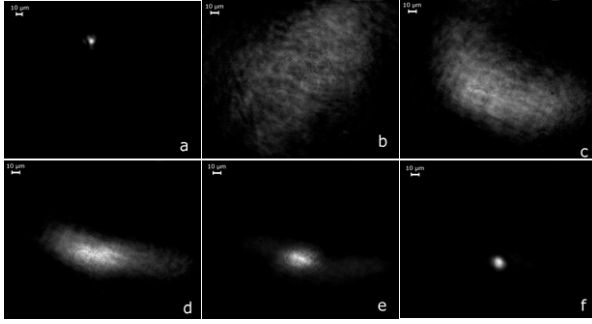


Fig. 5. Images of the beam spot at the input face (a) and at the output face of the crystal during the SWG writing process at different time steps. b-0min; c-5min; d-10min; e-15min; f-24min.

The SWG erasing time depends on the input beam wavelength and intensity. In our experiments, a SWG was erased using an input intensity of 2 kW/cm^2 (the same order of magnitude with the writing intensity) at $\lambda=532\text{ nm}$; the erasing time was about 80 minutes (Fig. 6). This brings a big advantage for the reconfigurability of the SWGs: the crystal allows the SWGs recording, erasing and recording again.

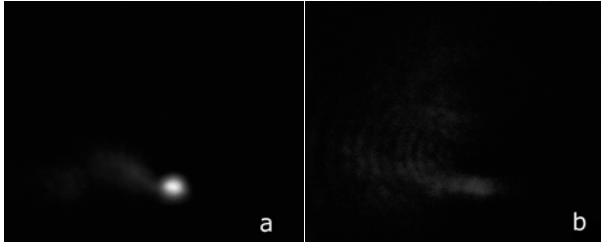


Fig. 6. SWG erasing by illuminating with 532nm radiation (a - 1 min, b - 77min).

4. SWG guiding properties

The guiding properties of SWGs were tested using cw. radiation (at $\lambda=532\text{ nm}$, $\lambda=808\text{ nm}$, $\lambda=1030\text{ nm}$, $\lambda=1557\text{ nm}$) and fs pulses ($\lambda=1030\text{ nm}$). The coupling was done translating laterally the LN crystal with respect to the incident beam direction.

In order to check the guiding properties, the images of the testing beam at the input and output faces of the crystal were acquired for the wavelengths mentioned above. These images are shown in Fig. 7. For $\lambda=1557\text{ nm}$, a different CCD camera, sensitive in IR, is used. It can be seen from the 2D beam profiles that the guiding properties are very good.

To better illustrate the guiding properties, the transversal section of the beam profile has been extracted from the beam spot images and fitted with a Gaussian function for the input profiles and with a square hyperbolic secant function for the output profiles. The results are shown in Fig. 8.

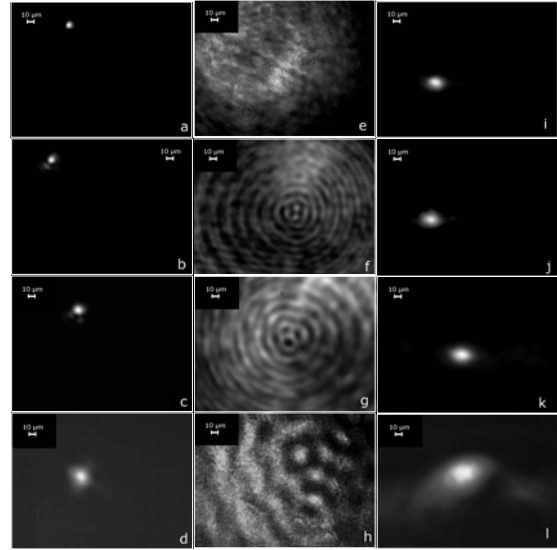


Fig. 7. Images of the beam spot at the crystal input face (a, b, c, d), at the output face, in free propagation through the LN crystal (e, f, g, h) and in guided propagation through SWG (i, j, k, l) at 532nm (a, e, i), 808nm (b, f, j), 1030nm (c, g, k), 1557nm (d, h, l).

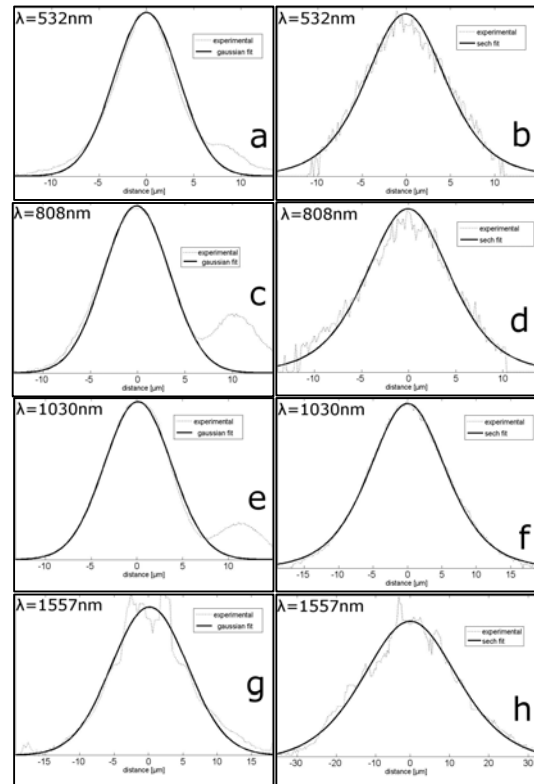


Fig. 8. Beam transversal profile at the input face (a,c,e,g) and output face (b,d,f,h) of the crystal.

For $\lambda=1557\text{ nm}$, the polarization of the light used for SWG writing has a significant influence on the guiding properties. We observed a better propagation in the SWGs

created with ordinary polarization, as was also reported in ref. [16]. This may be attributed to the higher refractive index contrast which can be obtained with this polarization.

The beam profiles for ultra-short pulses propagation are shown in Fig. 9. Comparing with Fig. 7, it can be seen that there is no major difference between c.w. and fs pulses propagation at this wavelength.

Dispersion calculations were made showing that at telecom wavelengths the LN material dispersion is very small. From our calculations and from other experimental results [21] the waveguide dispersion was found to be very small in comparison with material dispersion, so, only the material dispersion is of interest here.

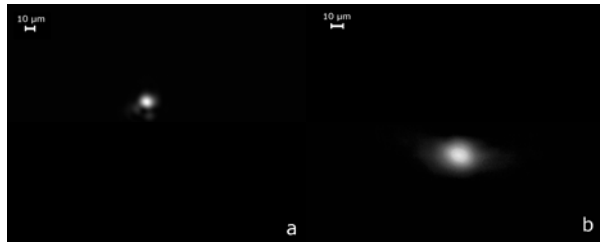


Fig. 9. Beam profile for fs pulses propagation at $\lambda=1030\text{nm}$ through the SWG:(a)-input profile; (b)-output profile.

The material dispersion coefficients, D_m , were calculated for different wavelengths of interest and are presented in Table 1.

Table 1. Material dispersion of LN.

λ [μm]	0.515	1.03	1.31	1.55
D_m [fs/(cm*nm)] Extraordinary	-57.26	-4.44	-1.77	-0.77
D_m [fs/(cm*nm)] Ordinary	-68.15	-5.12	-2.02	-0.87

We can calculate the temporal pulse broadening, $\Delta\tau$, using [22].

$$\Delta\tau = |D_m(\lambda)| \cdot z \cdot \Delta\lambda, \quad (3)$$

where z is the crystal length and $\Delta\lambda$ is the fs pulse wavelength bandwidth. For extraordinary polarization, $z=1\text{cm}$, $\Delta\lambda=3\text{nm}$ (for 300fs long pulses), the pulse broadening is $\Delta\tau=13.3\text{fs}$, for $\lambda=1.03\ \mu\text{m}$ and $\Delta\tau=2.3\text{fs}$, for $\lambda=1.55\ \mu\text{m}$.

5. Soliton waveguide array

There are three different methods for writing a soliton waveguide array which can have advantages or disadvantages as listed below.

A first method is to serially write the waveguides, process which can be computer controlled. The crystal is moved with desired spatial resolution at fixed time steps (representing the SWG writing time). This method can be tedious for bigger arrays but can also bring some advantage in decreasing the spatial resolution of the array. Also, the power required to write the array will be much decreased in contrast with a parallel writing method, in which the total required power should be the power required for recording of a SWG multiplied by the size (number of SWGs) of the array.

Another method is the parallel writing of the array. This can be done by using a diffractive optical element (DOE) [23] as a mask, a lens array, or using a spatial light modulator (SLM) [18]. The use of a fixed mask (a DOE or a lens array) does not allow the simple change of the distance between SWG. With a SLM there is a greater flexibility in choosing the array shape and distance between waveguides. The most desirable approach is probably a combination between the two methods to serially write smaller arrays to produce a big array if desired.

In this paper, we present a serially created SWG array of 13×10 solitons. We have adopted this method due to two main reasons, first for using a low-power laser and second, to test the SWG reproducibility. Considering the long propagation distance (15 diffractions lengths), the output beam diameter at the writing beginning is $150\ \mu\text{m}$. The spacing between SWGs was adjusted to $150\ \mu\text{m}$ horizontally and $100\ \mu\text{m}$ vertically. In this way, the solitons will not affect one each other in consecutive waveguide writing. The background illumination was the ambient laboratory light (fluorescent lamps) which was low enough to avoid the SWG erasing during the array recording.

The SWGs were individually visualized using a low power 532nm beam (around $4\ \mu\text{W}$) and the images were electronically superimposed in Fig. 10. The temporal stability of these SWGs is very good even without any additional fixing methods [24]. The images from Fig. 10 were obtained 2 months after the SWGs recording. The SWGs were also checked after 5 months using 1030nm radiation and the guiding properties remained very good.

6. Conclusions

In conclusion, we have demonstrated the possibility to create large SWG arrays in LN with good guiding properties and negligible dispersion at telecom wavelengths. This could lead to interesting soliton devices for ultra-fast parallel coupling and information processing in telecommunications. The writing process is simple and

also very cheap using low power lasers. By serially creating of this large array, we also showed a good reproducibility of the SWG writing process.

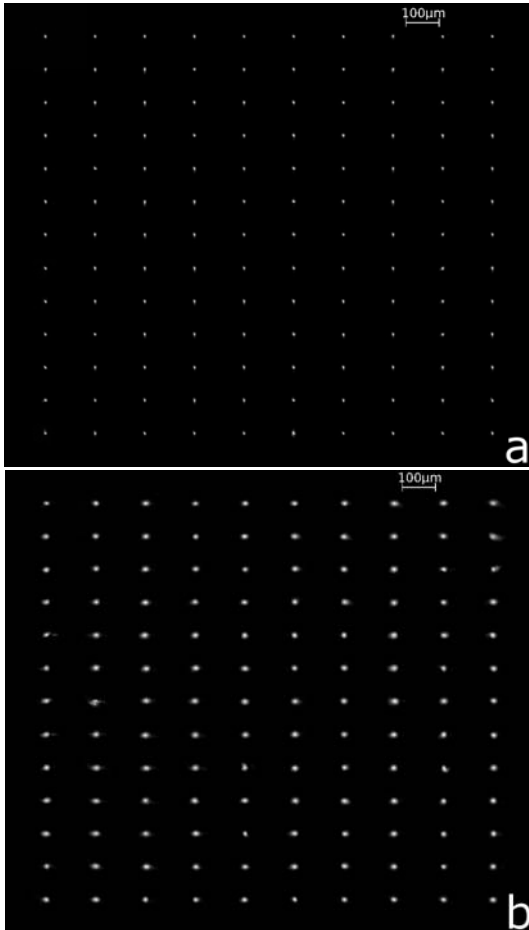


Fig. 10. 13x10 SWG array. (a) input; (b) output.

Acknowledgements

This work has been supported by the PNCDI 2 - IDEI project #572 (CNCSIS).

References

- [1] A. Askin, G. D. Boyd, J. M. Dziedzic, R. G. Smith, A. A. Ballman, J. J. Levinstein, K. Nassau, *Appl. Phys. Lett.* **9**, 72 (1966).
- [2] M. Segev, G. C. Valley, B. Crosignani, P. Di Porto, A. Yariv, *Phys. Rev. Lett.* **73**, 3211 (1994).
- [3] G. C. Duree, Jr., J. L. Shultz, G. J. Salamo, M. Segev, A. Yariv, B. Crosignani, E. J. Sharp, R. R. Neurgaonkar, P. Di Porto, *Phys. Rev. Lett.* **71**, 533 (1993).
- [4] Z. Chen, H. Martin, E. Eugenieva, J. Xu, J. Yang, *Opt. Express* **13**, 1816 (2005).
- [5] D. Kip, M. Wesner, V. Shandarov, P. Moretti, *Opt. Lett.* **23**, 921 (1998).
- [6] E. Fazio, F. Renzi, R. Rinaldi, M. Bertolotti, M. Chauvet, W. Ramadan, A. Petris, V. I. Vlad, *Appl. Phys. Lett.* **85**, 2193 (2004).
- [7] E. Fazio, W. Ramadan, A. Petris, M. Chauvet, A. Bosco, V.I. Vlad, M. Bertolotti, *Appl. Surf. Sci.* **248**, 97 (2005).
- [8] J. A. Andrade-Lucio, M. D. Iturbe-Castillo, P. A. Marquez-Aguilar, R. Ramos-Garcia, *Opt. Quantum Electron.* **30**, 829 (1998).
- [9] V. I. Vlad, E. Fazio, M. Bertolotti, A. Bosco, A. Petris, *Appl. Surf. Sci.* **248**, 484 (2005).
- [10] E. Fazio, V. Babin, M. Bertolotti, V. I. Vlad, *Phys. Rev. E* **66**, 016605 (2002).
- [11] E. Fazio, W. Ramadan, M. Bertolotti, A. Petris, V. I. Vlad, *J. Opt. A-Pure Appl. Opt.* **5**, 119 (2003).
- [12] E. Fazio, W. Ramadan, A. Belardini, A. Bosco, M. Bertolotti, A. Petris, V. I. Vlad, *Phys. Rev. E* **67**, 026611 (2003).
- [13] W. Ramadan, E. Fazio, A. Mascioletti, F. Inam, R. Rinaldi, A. Bosco, V. I. Vlad, A. Petris, M. Bertolotti, *J. Opt. A-Pure Appl. Opt.* **5**, 432 (2003).
- [14] G. Assanto, A. Fratolocchi, M. Peccianti, *Opt. Express* **15**, 5248 (2007).
- [15] K. Gallo, A. Pasquazi, S. Stivala, G. Assanto, *Phys. Rev. Lett.* **100**, 053901 (2008).
- [16] J. Safioui, M. Chauvet, F. Devaux, V. Coda, F. Pettazzi, M. Alonzo, E. Fazio, *J. Opt. Soc. Am. B* **26**, 487 (2009).
- [17] M. Petrovic, D. Träger, A. Strinic, M. Belic, J. Schröder, C. Denz, *Phys. Rev. E* **68**, 055601 (2003).
- [18] C. Denz, A. Desyatnikov, P. Jander, J. Schröder, D. Träger, M. Belic, M. Petrovic, A. Strinic, J. Petter, *Opt. Soc. Am.* **87**, 382 (2003).
- [19] T. Gorman, S. Haxha, *J. Lightwave Technol.* **25**, 3722 (2007).
- [20] M. Chauvet, V. Coda, H. Maillotte, E. Fazio, G. Salamo, *Opt. Lett.* **30**, 1977 (2005).
- [21] A. Petris, A. Bosco, V.I. Vlad, E. Fazio, M. Bertolotti, *J. Optoelectron. Adv. M.* **7**, 2133 (2005).
- [22] A. Ghatak, K. Thyagarajan, *Introducing to fiber optics* Cambridge University Press, 1999.
- [23] Z. Chen, K. McCarthy, *Opt. Lett.* **27**, 2019 (2002).
- [24] E. Fazio, M. Chauvet, V.I. Vlad, A. Petris, F. Pettazzi, V. Coda, M. Alonzo, P. Ferraro, S. Grilli, P. De Natale (Eds.), *Springer Series in Materials Science* **91**, Springer 2008.

*Corresponding author: silviu.popescu@inflpr.ro